



26 via Cinthia ed. 7

27 80126 Naples, Italia

28 Tel. +39 081 2534624

29 [giovanni.libralato@unina.it](mailto:giovanni.libralato@unina.it)

30

31

32

33 **Abstract**

34 This study assessed the effects and removal options of the macrolide spiramycin, currently  
35 used for both in human and veterinary medicine- with a special focus on advanced oxidation  
36 processes based on heterogeneous TiO<sub>2</sub>-assisted photocatalysis. Spiramycin real  
37 concentrations were investigated on a seasonal basis in a municipal wastewater treatment  
38 plant (up to 35 µg L<sup>-1</sup>), while its removal kinetics were studied considering both aqueous  
39 solutions and real wastewater samples, including by-products toxicity assessment. High  
40 variability of spiramycin removal by activated sludge treatments (from 9% (wintertime) to  
41 >99.9% (summertime)) was observed on a seasonal basis. Preliminary results showed that a  
42 total spiramycin removal (>99.9%) is achieved with 0.1 g L<sup>-1</sup> of TiO<sub>2</sub> in aqueous solution after  
43 80 min. Integrated toxicity showed residual slight acute effects in the photocatalytic treated  
44 solutions, independently from the amount of TiO<sub>2</sub> used, and could be linked to the presence of  
45 intermediate compounds. Photolysis of wastewater samples collected after activated sludge  
46 treatment during summer season (SPY 5 µg/L) allowed a full SPY removal after 80 min.  
47 When photocatalysis with 0.1 g L<sup>-1</sup> of TiO<sub>2</sub> was carried out in wastewater samples collected in  
48 winter season (SPY 30 µg L<sup>-1</sup>) after AS treatment, SPY removal was up to 91% after 80 min.

49

50 **Keywords**

51 Advanced oxidation processes; mass spectrometry; antibiotics; TiO<sub>2</sub>; toxicity

52

53 **Highlights**

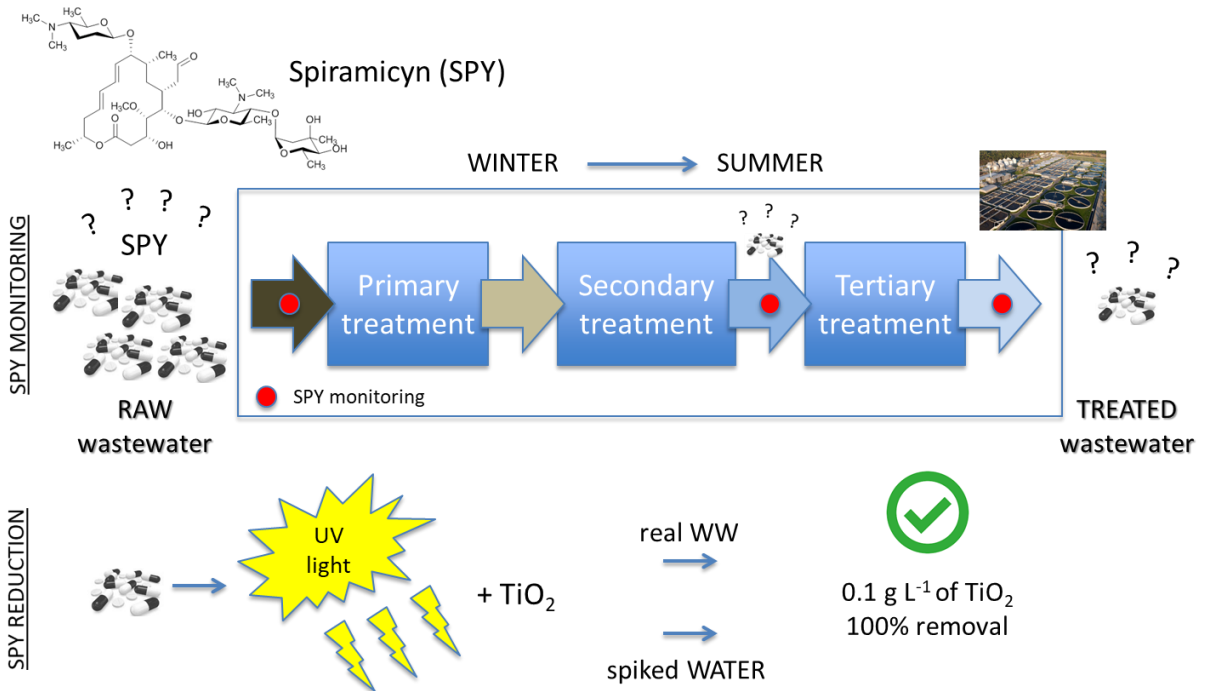
54

- 55 • SPY in WWTP before and after wastewater treatment was up to 35 µg L<sup>-1</sup>
- 56 • SPY reduction was more effective in summer than winter by AS treatment
- 57 • Photocatalysis (winter samples) (0.1 g TiO<sub>2</sub> L<sup>-1</sup>, 80 min) reduced SPY up to 91%

58

- After treatment, ecotoxicity was 7-18% due to residual oxidation by-products

# 59 Graphical Abstract



60  
61  
62  
63  
64

## 65 **1. Introduction**

66 Antibiotics released into the environment through the wastewater cycle are considered  
67 contaminants of emerging concern belonging to the class of micro- and nano-pollutants  
68 similarly to engineered nanomaterials (Minetto et al., 2016), textile dyes and other textile by-  
69 products and personal care residues (Lofrano et al., 2016a; Libralato et al., 2011).

70 In the European Union between 2010 and 2014, the overall human antibiotic consumption  
71 showed a significant increasing trend with a large inter-country dissimilarity (i.e. from 1.1  
72 packages/1000 inhabitants per day in Sweden up to 3.8 packages/1000 inhabitants per day in  
73 Italy) (ECDC, 2014). Sarmah et al. (2016) stated that veterinary antibiotics might play a  
74 leading role in wastewater contamination largely contributing to the final load of drugs  
75 discharged into the environment on a specific geographical basis (e.g. presence of intensive  
76 livestock breeding). According to Wang and Tang (2010), the total worldwide amount of used  
77 antibiotics (medical and veterinary) reached up to  $2 \cdot 10^5$  ton/y. The consumption of  
78 antimicrobials by livestock is expected to increase from  $63151 \pm 1560$  ton in 2010 to  $105596$   
79  $\pm 3605$  ton in 2030 (Van Boeckel et al., 2015). As antibiotics are poorly adsorbed in animal  
80 guts, a great part of them is excreted into faeces and urine, and, frequently, in a form that is  
81 not metabolized. When zootechnical wastewater is discharged into sewage (i.e. with or  
82 without *in situ* pre-treatment) and subsequent into municipal wastewater treatment plants  
83 (WWTPs), a significant increase in the antibiotic load is expected at the influent (Sarmah et  
84 al., 2016). Indeed, several studies showed that conventional WWTPs could not completely  
85 remove antibiotics, thus, they can finally enter the aquatic and terrestrial environment via  
86 conventional effluent and sewage sludge disposal (Watkinson et al., 2007; Batt et al., 2007;  
87 Zuccato et al., 2010; Gracia-Lor et al., 2012; Michael et al., 2013; Birošová et al., 2014).  
88 According to Zuccato et al. (2010), wastewater samples from northern Italy WWTPs (Milan,  
89 Como and Varese) presented an amount of antibiotics ranging within 115–237 g per 1000

90 inhabitants per year in both influent and effluent and, thus, being potentially released into the  
91 receiving water bodies. Macrolides, particularly clarithromycin, spiramycin, and quinolones  
92 are the most abundant antibiotics in untreated wastewater. After penicillin and quinolones,  
93 ECDC (2014) estimated that macrolides are the third class of antibiotics consumed in Italy.  
94 Antibiotics both taken singly and as mixtures showed to influence both the structure and  
95 function of algal communities (Wilson et al., 2003). They showed to influence the  
96 development, transfer, or spread of antibiotics resistant bacteria and/or antibiotics resistant  
97 genes in a long-term perspective (Ferro et al., 2015). They can impair human embryonic cells  
98 and affect zebrafish liver cells proliferation (Pomati et al., 2006, 2007), but data are still  
99 scarce for (environmental) risk assessment.

100 The environmental concern associated to the release of antibiotics in the aquatic ecosystems is  
101 expected to increase over time especially when considering the reuse of conventionally  
102 treated wastewater (e.g. industry, hospital and household) increasing the risk of drinking  
103 water contamination and, thus, non-voluntary human exposure (Kim and Aga, 2007; Benotti  
104 et al., 2008). Consequently, the European Commission updated the Watch List of substances  
105 for Union-wide monitoring (Commission Implementing Decision 2015/495) including  
106 erythromycin, clarithromycin, and azithromycin.

107 To face up the antibiotic removal, the performance of traditional activated sludge (AS)  
108 WWTP should be improved including further treatments like advanced oxidation processes  
109 (AOPs) such as ozonation, Fenton, photo-Fenton oxidation, and heterogeneous photocatalysis  
110 that are gaining growing interest as complementary treatments (De Luca et al., 2013;  
111 Carotenuto et al., 2014; Lofrano et al., 2016b; Lofrano et al., 2017; Rasheed et al., 2017a;  
112 Rasheed et al., 2017b). Amongst AOPs, TiO<sub>2</sub>-assisted photocatalysis is being considered as  
113 an effective and sustainable technology for the degradation and detoxification of complex  
114 organic chemicals (Vaiano et al., 2015). The photocatalytic process consists in utilizing the

115 ultra-violet (UV) irradiation ( $\lambda < 380$  nm) to photoexcite a semiconductor catalyst in presence  
116 of oxygen. Within this scenario, oxidizing species (i.e. bound hydroxyl radical ( $\bullet\text{OH}$ ) or free  
117 holes) attack oxidable substances producing a progressive breaking down of macro-molecules  
118 yielding to  $\text{CO}_2$ ,  $\text{H}_2\text{O}$  and diluted inorganic acids. The most commonly used catalyst is the  
119 semiconductor  $\text{TiO}_2$ , mainly because it is an abundant, non-expensive, and relatively low  
120 toxic product (Malato et al., 2002).

121 Nevertheless the huge amount of papers about AOPs, gaps into the knowledge about the  
122 proper management of antibiotics in wastewater treatment is still present mainly due to the  
123 absence of toxicity identification evaluation of treated effluents that only rarely consider a  
124 complete battery of toxicity tests and final toxicity data integration. Scarce information exists  
125 about spiramycin (SPY) behaviour in wastewater. SPY is a macrolide antibiotic widely used  
126 to treat human (e.g. oropharynx, respiratory system, and genito-urinary tract) and veterinary  
127 infections (e.g. cryptosporidiosis and toxoplasmosis). This research investigated on a seasonal  
128 basis SPY presence in wastewater samples collected before and after treatment in a municipal  
129 AS WWTP (Campania Region, Italy) to monitor the state-of-the-art and assess the  
130 potentiality for its reduction/removal at real scale via AOPs. The photocatalytic degradation  
131 of SPY was evaluated by using a range of  $\text{TiO}_2$  concentrations both in biologically treated  
132 wastewater samples and aqueous solutions. Photo-degradation by-products were investigated,  
133 and toxicity of samples using a full battery of bioassays was provided to complete the  
134 characterization of the performance of the treatment process.

135

## 136 **2 Materials and methods**

### 137 **2.1 Wastewater treatment plant and sampling**

138 Samples were collected from a municipal WWTP, located in Campania region (Italy)  
139 receiving wastewater collected from urban households, agro-industries, zootechnical

140 activities, hospices and other facilities. The WWTP had an average capacity of 300 000 p.e.,  
141 and a flow rate ranging between 30 000 m<sup>3</sup> d<sup>-1</sup> (winter) up to 60 000 m<sup>3</sup> d<sup>-1</sup> (summer) due to  
142 seasonal activities (e.g. cannery industries). The treatment process includes: i) Mechanical  
143 pre-treatment (screening and pumping stations, grit and oil removal); ii) Rainwater section  
144 (primary sedimentation and aerated storage); iii) Secondary treatment (nitrification-  
145 denitrification and final settling); and iv) Tertiary treatment (gravity filtration on sand), and  
146 disinfection with peracetic acid.

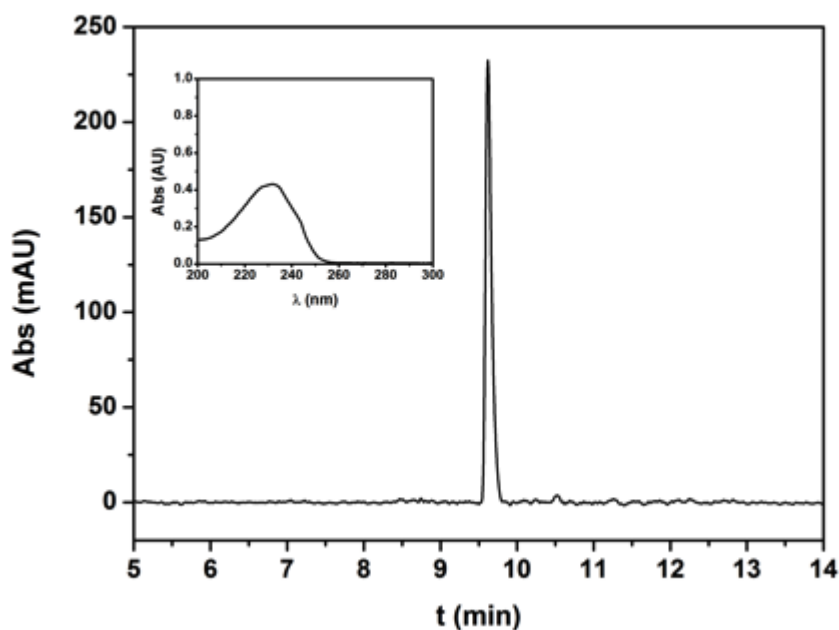
147 Two weeks seasonal sampling campaigns were carried out at the WWTP in winter and  
148 summer 2015 with three sampling points: i) influent; ii) wastewater after the biological  
149 treatment; iii) effluent. Samples were collected three times per day and mixed to obtain a  
150 composite sample. During sampling, no rainfall events were registered and daily WWTPs  
151 hydraulic loading rates were nearly constant. Samples were kept at 4 °C in the darkness during  
152 the way back to the laboratory. Wastewater were characterised for COD, TSS, NH<sub>3</sub>, NO<sub>3</sub>,  
153 NO<sub>2</sub>, according to APHA (2012).

154

## 155 **2.2 Materials and analytical procedures**

156 SPY (Sigma-Aldrich) presents high solubility in water and is freely soluble in ethanol 96%  
157 (C<sub>43</sub>H<sub>74</sub>N<sub>2</sub>O<sub>14</sub>; 443.053 g mol<sup>-1</sup>; solid appearance: white or yellow-white powder). We  
158 selected the P25 TiO<sub>2</sub> (80% anatase and 20% rutile) for heterogeneous photocatalysis  
159 (Evonik, Essen, Germany). Sigma Aldrich (Sant Louis, MO, USA) supplied high performance  
160 liquid chromatography (HPLC) grade water, methanol, acetonitrile and formic acid. The  
161 ultraviolet–visible (UV-Vis) spectra were recorded using a spectrophotometer (Varian, Cary  
162 50). The degradation of SPY dispersed in ultra-pure water was followed by HPLC-UV  
163 (Finnigan Surveyor LC Pump Plus, USA) equipped with a reversed phase C18 analytical  
164 column (Phenomenex Luna, 3 µm, 2.1 mm × 150 mm) with UV-Vis spectrophotometer

165 (Finnigan Surveyor UV-VIS Plus Detector, USA). The compound was eluted using as mobile  
166 phase a mixture of 0.1% formic acid in water (eluent A) and 0.1% formic acid in acetonitrile-  
167 methanol (1:1 v:v) (eluent B) at a flow rate of 0.2 mL min<sup>-1</sup>. The initial concentration was  
168 10% B followed by a linear gradient from 10 to 70% B over the course of 3 min and 80%  
169 over the next 2 min. Finally, eluent B was lowered to 10 % in 1 min. Before the next  
170 injection, the system could equilibrate for 9 min. The injection volume was 20 µL and the  
171 wavelength set for the quantification was 230 nm according to the maximum light absorption  
172 of SPY (inlet Fig. 1). Under these conditions, the retention time of SPY was about 9.7 min  
173 (Fig.1). The limit of quantification (LOQ) was 0.1 µg mL<sup>-1</sup>. Data were collected by  
174 ChromQuest version 3.1.6 software (Thermo Electron 2003). The quantification of SPY in  
175 wastewater was performed using an LC-MS equipped with a 1525 binary pump (Waters,  
176 Milford, MA, USA) and a Phenomenex Luna-C18 column (3 µm, 2.1 mm × 150 mm). The  
177 eluents and the condition were the same used for the HPLC analysis Before the next injection,  
178 the system could equilibrate for 4 min. The injection volume was 10 µL. Under these  
179 conditions, the retention time of SPY was 5.8 min (Fig. 1S). The limit of quantification  
180 (LOQ) was equal to 0.1 ng mL<sup>-1</sup>.



181  
182 **Figure 1** HPLC chromatogram of SPY; (inlet) UV spectra of SPY.  
183  
184 A Quattro micro API (Micromass, Manchester, UK) triple quadrupole tandem mass  
185 spectrometer operating in the multiple reaction monitoring (MRM) positive ion mode was  
186 used for SPY detection in wastewater. Data acquisition was accomplished by MassLynx  
187 version 4.1 software (Micromass, Manchester, UK). The following conditions were found to  
188 provide the optimum signal: ion source temperature, 100 °C; desolvation temperature, 250 °C;  
189 cone gas, 30 L h<sup>-1</sup>; desolvation gas, 500 L h<sup>-1</sup>; cone voltage, 20 V; collision energy, 10 eV;  
190 and capillary voltage, 3.0 kV. One MRM transitions were analysed: 422.3–176.0 m z<sup>-1</sup>.  
191 Quantification was accomplished using an external standard method. Instrument calibration  
192 included the analysis of standards at 10, 100, 500, 1000 nmol L<sup>-1</sup>. A blank sample was  
193 analyzed between each sample to verify that the measured SPY concentrations were not false  
194 positives.  
195 For the by-products identification mass spectra were acquired with a Bruker solarix XR  
196 Fourier transform mass spectrometer (Bruker Daltonik GmbH, Bremen, Germany) equipped

197 with a 7T refrigerated actively shielded superconducting magnet (Bruker Biospin,  
198 Wissembourg, France). The samples were ionized in positive ion mode using ESI (Bruker  
199 Daltonik GmbH, Bremen, Germany).

200 Sample solutions were continuously supplied using a syringe pump at a flow rate of  $120 \mu\text{L h}^{-1}$ .  
201 The detection mass range was set to 100-1000  $\text{m z}^{-1}$ . The mass spectra were calibrated  
202 externally with a solution of sodium trifluoroacetate in water in positive ion mode using a  
203 linear calibration.

204

### 205 **2.3 Experimental plan**

206 A first set of investigation was aimed at evaluating the effects of  $\text{TiO}_2$  in dark conditions to  
207 set the background level of SPY removal and potential adsorption. Two concentrations of  
208 SPY (10 and  $70 \text{ mg L}^{-1}$ ) were selected to evaluate the influence of the initial antibiotic  
209 concentration, in addition the solution at  $70 \text{ mg L}^{-1}$  SPY was used to facilitate the  
210 identification of the potential oxidation by-products. Photolysis experiments were carried out  
211 at  $20^\circ\text{C}$  in a 250 mL magnetic stirred cylindrical Pyrex vessel filled with 200 mL of ultra-  
212 pure water solution ( $10\text{-}70 \text{ mg L}^{-1}$  of SPY). In photocatalysis experiments, various  $\text{TiO}_2$   
213 concentrations (0.1, 0.5, 1, 2 and  $4 \text{ g L}^{-1}$ ) were added to the same solutions ( $10\text{-}70 \text{ mg L}^{-1}$  of  
214 SPY) at natural  $\text{pH} = 5.5$ .

215 The reaction vessel was placed in a chamber and illuminated for 5, 10, 20, 40, and 80 min  
216 with a xenon arc lamp (450 W, Lot Oriel Group, Italy) equipped with special glass filtering  
217 the transmission of wavelengths below 320 nm to use the radiation able to activate the  
218 catalyst. The irradiation was determined by the potassium ferrioxalate actinometry (Hatchard  
219 and Parker, 1956) was  $4.5 \times 10^{-7} \text{ Einstein s}^{-1}$ . After the photocatalysis process, samples were  
220 slowly filtered through  $0.45 \mu\text{m}$  pore size mixed esters membrane (Millipore, Billerica, MA,  
221 USA) to remove the catalyst. Dark experiments were carried out with the lamp switched off.

222 Finally, dark photolysis and photocatalysis experiments were carried out on the samples from  
223 the effluent of the biological treatment during summer and winter seasons, once the optimum  
224 TiO<sub>2</sub> concentration was determined.

225

#### 226 **2.4 Ecotoxicity and data analysis**

227 Toxicity was investigated in accordance to Lofrano et al. (2016) via a battery of acute (A) and  
228 chronic (C) toxicity tests including biological models belonging to various trophic levels like  
229 *Vibrio fischeri* (A), *Raphidocelis subcapitata* (C), and *Daphnia magna* (A). Toxicity tests  
230 were carried out on untreated 10 mg L<sup>-1</sup> SPY solution (pure substance) and after the  
231 photocatalytic treatment with various TiO<sub>2</sub> concentrations (0.1, 0.5, 1, 2 and 4 g L<sup>-1</sup>) for 80  
232 min. Toxicity tests with *V. fischeri* (NRRL-B-11177) were carried out according to ISO  
233 (2008). The luminescence was measured with a Microtox® analyzer (Model 500, AZUR  
234 Environmental) after 5 and 15 min at 15 °C. Tests were carried out in triplicate. Data were  
235 analysed with Microtox Omni® software and the result expressed as percentage of  
236 bioluminescence inhibition (%). Microalgae growth inhibition test with *R. subcapitata* was  
237 carried out according to ISO (2012). Cultures were kept in Erlenmeyer flasks. The initial  
238 inoculum contained 10<sup>4</sup> cells mL<sup>-1</sup>. The specific growth inhibition rate was calculated  
239 considering 6 replicates exposed at 20 ± 1 °C for 72 h under continuous illumination (6000  
240 lx). Effect data were expressed as percentage of growth inhibition. Toxicity tests with *D.*  
241 *magna* were carried out according to ISO (2013) and Maselli (2017). Newborn daphnids (<  
242 24 h old) were exposed in four replicates for 24 and 48 h at 20 ± 1 °C under continuous  
243 illumination (1000 lx). Before testing, they were fed with *R. subcapitata* (300,000 cells mL<sup>-1</sup>)  
244 *ad libitum*. Toxicity was expressed as the percentage of dead organism and corrected for the  
245 effects in negative controls (0 g/L TiO<sub>2</sub>) according to Abbott's formula. All toxicity tests  
246 included the assessment of negative and positive controls in accordance with the specific

247 reference method. Toxicity was expressed as percentage of effect or as effective concentration  
248 causing the 5 (EC5), 20 (EC20) and 50% (EC50) effect to the exposed population. After the  
249 verification of homoschedasticity (F test,  $p < 0.05$ ) and normality (Shapiro-Wilk test,  $p <$   
250  $0.05$ ) of toxicity data, the significance of differences between average values of different  
251 experimental treatments and controls was assessed by the analysis of variance (ANOVA,  $p <$   
252  $0.05$ ). When ANOVA revealed significant differences among treatments, *post-hoc* tests were  
253 carried out with Tukey's test ( $p < 0.05$ ). Statistical analyses were performed using Microsoft®  
254 Excel 2013/XLSTAT©-Pro (Version 7.2, 2003, Addinsoft, Inc., Brooklyn, NY, USA).  
255 Toxicity data have been integrated according to Persoone et al. (2003) approach for natural  
256 water. According to Libralato et al. (2010) and Lofrano et al. (2016), the hazard classification  
257 system based on percentage of effect (PE) includes a Class I for  $PE < 20\%$  (score 0), Class II  
258 for  $20\% \leq PE < 50\%$  (score 1), Class III for  $50\% \leq PE < 100\%$  (score 2), Class IV when  $PE =$   
259  $100\%$  in at least one test (score 3) and a Class V when  $PE = 100\%$  in all bioassays (score 4).  
260 Finally, the integrated class weight score was determined by averaging the values  
261 corresponding to each microbiotest class normalised to the most sensitive organism (highest  
262 score).

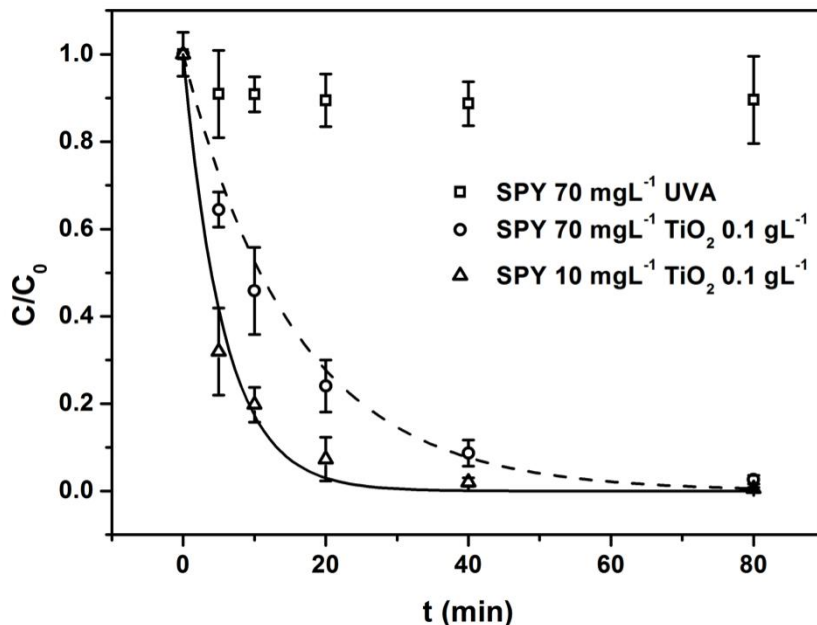
### 263 **3 Results and discussion**

#### 264 **3.2 Heterogeneous photocatalysis of SPY in aqueous solutions**

##### 265 **3.2.1 Effect of SPY concentration**

266 Screening experiments carried out in the dark at  $10 \text{ mg L}^{-1}$  and  $70 \text{ mg L}^{-1}$  of SPY in distilled  
267 water considering a concentration equal to  $0.1 \text{ g L}^{-1}$  of  $\text{TiO}_2$  proved that adsorption was  
268 negligible in the antibiotic removal (data not shown). As reported in Figure 2, a slight  
269 decrease in SPY concentration could be observed during photolysis experiments. After 80  
270 min of irradiation, antibiotic removal was set at 11% for  $70 \text{ mg L}^{-1}$  of SPY. As for most of the  
271 organic compounds, SPY photolysis resulted strongly influenced by both the wavelength and

272 intensity of UV source (Lofrano et al., 2016b). Chekir et al. (2013) reported a SPY ( $10 \text{ mg L}^{-1}$ )  
273 removal  $< 7\%$  after 6 h of irradiation with 2 Phillips lamps (PL-L 24 W/10/4P;  $\lambda_{\text{max}} = 365$   
274 nm).



275  
276 **Figure 2** Photocatalytic kinetic curves of SPY ( $10$  and  $70 \text{ mg L}^{-1}$ ) after 5, 20, 40, 80 min at  
277  $0.1 \text{ g L}^{-1}$  of  $\text{TiO}_2$  at pH 5.5; error bars represent standard error ( $n = 3$ ).

278  
279 According to Calza et al. (2010), the complete disappearance of the drug ( $15 \text{ mg L}^{-1}$ ) occurred  
280 through a pseudo-first-order decay (1,500-W Xenon lamp equipped with a 340-nm cut-off  
281 filter simulating AM1 solar light). In sterilised water,  $t_{1/2}$  was 48 h, further reduced to 25 h  
282 when SPY was spiked in river water.

283 In photocatalysis experiments, the action of  $0.1 \text{ g L}^{-1}$  of  $\text{TiO}_2$  combined with UV radiation  
284 after 80 min increased the reduction up to 99% and 97% for  $10 \text{ mg L}^{-1}$  and  $70 \text{ mg L}^{-1}$  of SPY,  
285 respectively. Antibiotic reduction was faster at  $10 \text{ mg L}^{-1}$  of SPY. The degradation rate was  
286 inversely dependent to the initial SPY concentration following the pseudo-first-order kinetic  
287 model: i)  $k = 0.17 \pm 0.02 \text{ min}^{-1}$ ,  $t_{1/2} = 4.0 \pm 0.4 \text{ min}$  at  $10 \text{ mg L}^{-1}$  of SPY; ii)  $k = 0.064 \pm 0.003$   
288  $\text{min}^{-1}$ ,  $t_{1/2} = 10.8 \pm 0.5 \text{ min}$  at  $70 \text{ mg L}^{-1}$  of SPY. Similarly, Chekir et al. (2013) reported

289 reduction rates equal to 95.6%, 89.9%, and 78.4% for 10, 20, 40 mg L<sup>-1</sup> of SPY, respectively,  
290 under simulated sunlight after 360 min with 0.25 g L<sup>-1</sup> of TiO<sub>2</sub>.

291

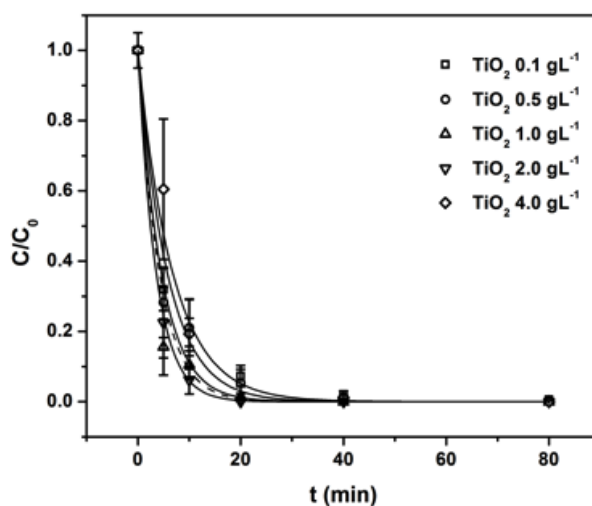
### 292 **3.2.2 Effect of catalysts in SPY aqueous solution**

293 In order to evaluate the catalyst effect, several loads (0.1, 0.5, 1, 2, 4 g L<sup>-1</sup> of TiO<sub>2</sub>) were  
294 tested in photocatalysis of 10 mg L<sup>-1</sup> of SPY. After 80 min of photo-oxidation, significant  
295 SPY removal (> 99.9%) was achieved with 0.1 g L<sup>-1</sup> of TiO<sub>2</sub> (Figure 3). During treatment,  
296 SPY reduction increased with TiO<sub>2</sub> concentration up to a degradation of >99.9% using 2 g L<sup>-1</sup>  
297 of TiO<sub>2</sub> after 10 min of contact time. A complete SPY removal was achieved as well after 40  
298 min of photo-degradation with 1 g L<sup>-1</sup> of TiO<sub>2</sub>. Beyond this value, the degradation remained  
299 approximately constant and the rate constant evolution was low. Above 2 g L<sup>-1</sup> of TiO<sub>2</sub>,  
300 particles caused a shadowing effect reducing the penetration ability of the radiation, thus  
301 reducing the formation of hydroxyl radicals being responsible of SPY oxidation. Chekir et al.  
302 (2013) achieved a 96% SPY removal (10 mg L<sup>-1</sup>) after 360 min of photo-oxidation using 0.25  
303 g L<sup>-1</sup> of TiO<sub>2</sub>.

304 The optimum TiO<sub>2</sub> concentration must be determined time-by-time to avoid the use of an  
305 excess of the reactive agent ensuring that the absorption of radiation photons is maximized for  
306 an efficient degradation (Lofrano et al., 2016b).

307 The photocatalytic reduction of SPY (10 mg L<sup>-1</sup>) followed a pseudo first order (PFO) kinetic  
308 equation, corresponding to photocatalytic degradation rate constants reported in Table 2 with  
309 the half-life (t<sub>1/2</sub>) values.

310



311  
 312 **Figure 3** Photocatalytic kinetic curves of SPY ( $10 \text{ mg L}^{-1}$ ) after 5, 10, 20, 40, 80 min at 0.1,  
 313 0.5, 1.0, 2.0, 4.0  $\text{g L}^{-1}$  of  $\text{TiO}_2$  at pH 5.5; error bars represent standard error ( $n = 3$ ).

314  
 315 **Table 2** Half-life ( $t_{1/2}$ ) of SPY ( $10 \text{ mg L}^{-1}$ ) and the pseudo first order constant ( $k$ ) .

$\text{TiO}_2$	$t_{1/2}$	$k$
$\text{g L}^{-1}$	min	$\text{min}^{-1}$
0.1	$4.0 \pm 0.4$	$0.180 \pm 0.020$
0.5	$4.7 \pm 0.2$	$0.148 \pm 0.006$
1.0	$3.1 \pm 0.3$	$0.220 \pm 0.020$
2.0	$2.5 \pm 0.1$	$0.282 \pm 0.006$
4.0	$2.9 \pm 0.3$	$0.240 \pm 0.030$

316  
 317

318 **3.2.3 Degradation products**

319 Degradation products may promote microbial resistance, above all if the active part of the  
320 molecule remains unmodified, and/or generate more toxic effects than their parent  
321 compounds. Consequently, monitoring not only drug degradation but also its metabolites is of  
322 increasing relevance in evaluating their environmental impact. Calza et al. (2010) reported  
323 that most transformation products formed after photocatalytic treatment of 15 mg L<sup>-1</sup> SPY  
324 with 0.1 g L<sup>-1</sup> of TiO<sub>2</sub> reached their maximum amounts up to 15 min of irradiation. Some of  
325 them (m/z 526, 859,699) were removed after 60 min, whereas the smaller molecules (m/z  
326 144, 160,176, 336) took more time to be degraded disappearing only after 120 min. A similar  
327 behaviour was observed in the present study, monitoring the transformation products as a  
328 function of the irradiation time.

329 Figure 4 reports the ESI-MS spectra on untreated SPY (70 mgL<sup>-1</sup>) and photocatalysis-treated  
330 solutions with 0.1 gTiO<sub>2</sub> L<sup>-1</sup> over the time. The ESI-MS spectra showed a progressive  
331 degradation of SPY and the formation of several intermediates and/or by-products after 10  
332 min of photocatalysis the m/z 143, 175, 335, 525, 698, 701, 814, 828, 859, 891, were detected  
333 and after 20 min the m/z 159 appeared. The molecules associated to the peaks identified in  
334 Figure 4 are shown in Figure 5. All of them were still present after 80 min of photocatalysis.

335

336

337

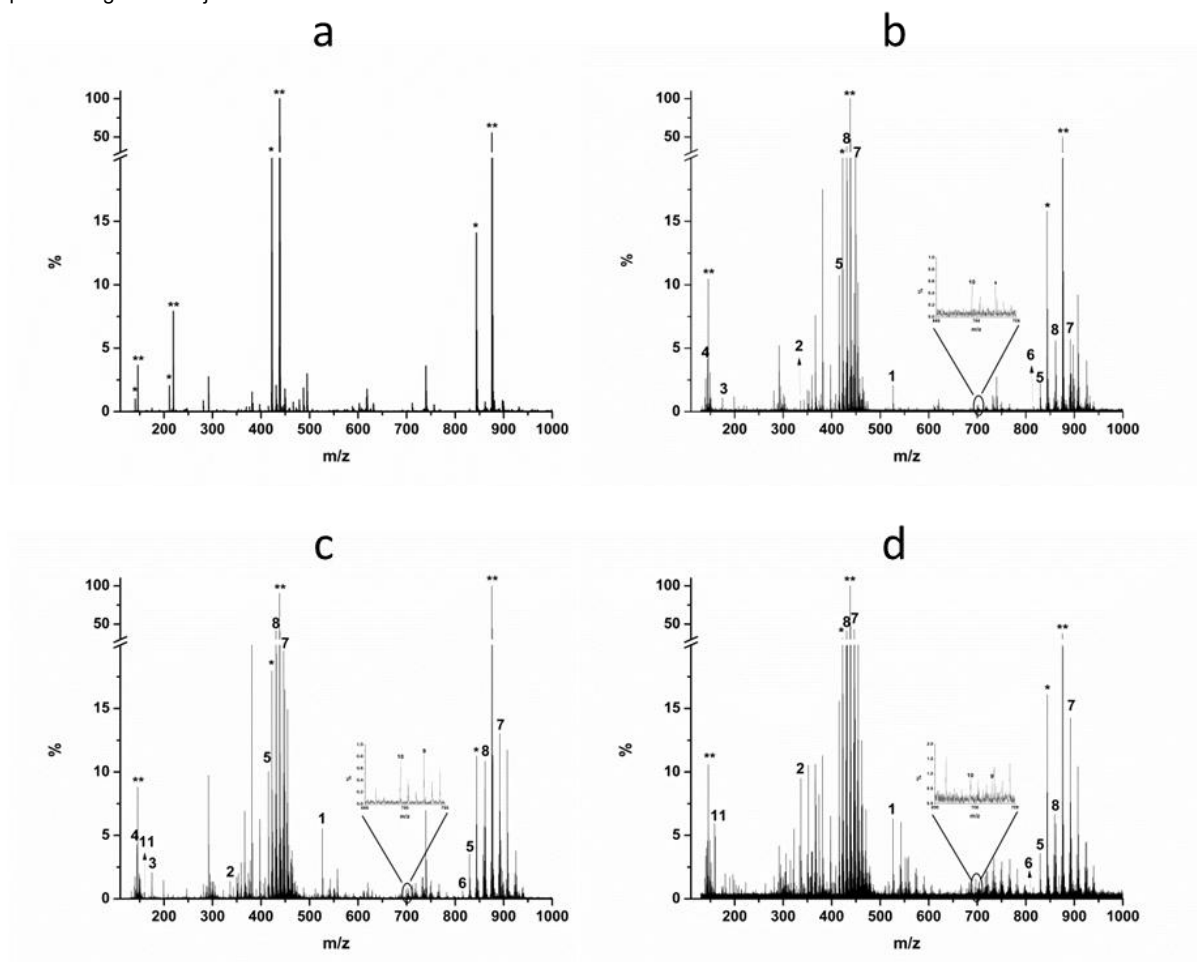
338

339

340

341

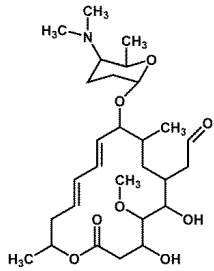
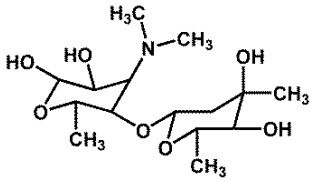
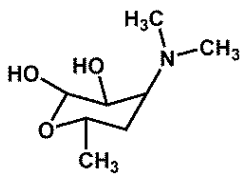
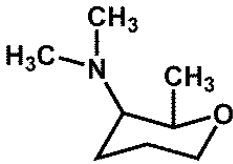
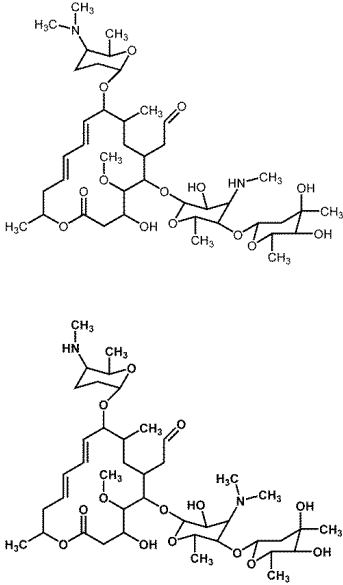
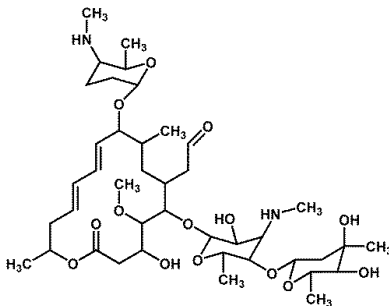
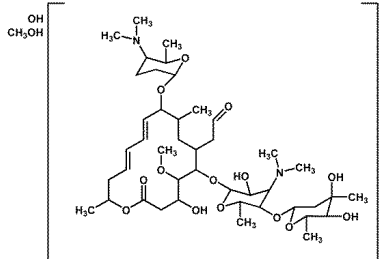
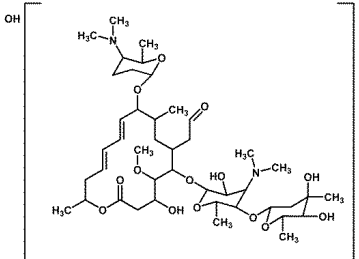
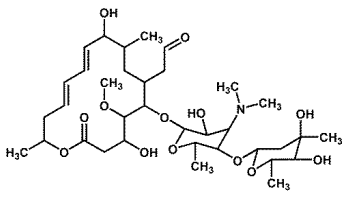
342

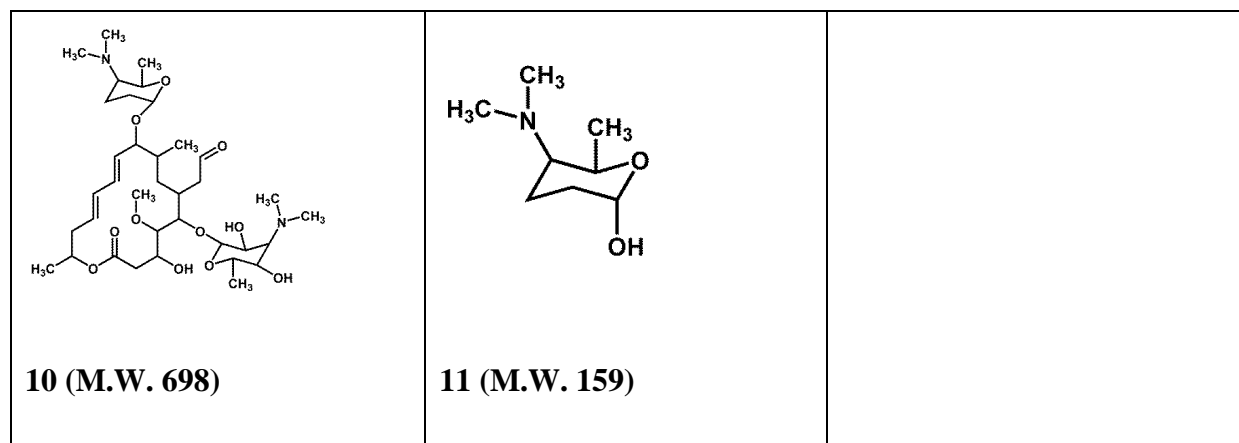


343

344 **Figure 4** ESI-MS spectra in positive ion mode on untreated SPY ( $70 \text{ mgL}^{-1}$ ) (a), SPY  
345 photocatalysis ( $70 \text{ mgL}^{-1}$ ) at  $0.1 \text{ gL}^{-1}$  of  $\text{TiO}_2$  after 10 min (b), 20 min (c) and 80 min (d);  
346 \*SPY and \*\* [SPY +  $\text{CH}_3\text{COOH}$ ] formed during the injection phase in ESI-MS.

347

 <p><b>1 (M.W. 525)</b></p>	 <p><b>2 (M.W. 335)</b></p>	 <p><b>3 (M.W. 175)</b></p>
 <p><b>4 (M.W. 143)</b></p>	 <p><b>5 (M.W. 828)</b></p>	 <p><b>6 (M.W. 814)</b></p>
 <p><b>7 (M.W. 891)</b></p>	 <p><b>8 (M.W. 859)</b></p>	 <p><b>9 (M.W. 701)</b></p>



348

349 **Figure 5** Molecules associated to the peaks identified in Figure 4.

350

351 **3.1 Occurrence and removal of SPY in WWTP**

352 Real SPY concentrations detected in wastewater samples are reported in Table 1. Wintertime  
 353 showed a significantly higher presence of SPY compared to summertime. In winter, the  
 354 average SPY concentration was 32  $\mu\text{g L}^{-1}$  in both influent and effluent specimen thus being  
 355 significantly higher than the average concentrations of SPY measured in effluents from nine  
 356 Italian WWTPs (75  $\text{ng L}^{-1}$ ) (Zuccato et al., 2005). Birošová et al. (2016) observed a similar  
 357 trend highlighting higher levels of antibiotics in raw wastewater samples from two Bratislava  
 358 WWTPs (Slovakia) in February than in August. The clarithromycin concentration ranged  
 359 from 0.7  $\mu\text{g L}^{-1}$  in August up to 2.520  $\mu\text{g L}^{-1}$  in February. McArdell et al. (2003) reported that  
 360 winter antibiotic concentrations might be two times higher than in summertime.

361

362 **Table 1** Occurrence of SPY in WWTP (Campania, Italy) before (influent), after activated  
 363 sludge (AS) biological treatment and at the final discharge point (effluent); SPY reduction  
 364 rates (%) were reported within the same season ( $\text{RR}_W$  = Reduction Rate influent-effluent) and  
 365 between winter- and summertime ( $\text{RR}_B$ ).

	Influent	After AS treatment	Effluent	$\text{RR}_W$
	$\mu\text{g L}^{-1}$			%
Winter (February)	35 ± 7	34 ± 7	32 ± 7	9
Summer (July)	5 ± 2	< 0.1	< 0.1	>99.9%
$\text{RR}_B$ (%)	86%	>99.9%	>99.9%	-

366

367 Municipal WWTPs are the major pathway for the disposal of antibiotics, and the  
368 concentrations measured in influent can reflect the levels of antibiotics in its collection area  
369 (Al-Rifai et al., 2011; Jelić et al., 2009, Li et al., 2013). Li et al. (2011) observed as the sums  
370 of the average daily mass flow of antibiotics from influent of two WWTPs in Hong Kong  
371 changed significantly according to the living standard of the serving regions even in the same  
372 city. Thus, the higher value detected in winter samples could be partially attributed to the  
373 higher frequency of antibiotic prescription in Campania Region and/or its misuse (i.e. the  
374 higher SPY consumption during winter caused by the higher amount of potential infections  
375 and the lower ability of WWTPs in wintertime to effectively reduce/remove such a highly  
376 concentrated and recalcitrant compound due to low environmental temperatures).

377 In the surroundings of the WWTP, there are no pharmaceutical industries or hospitals and,  
378 thus, the average concentrations could reflect mainly the domestic antibiotic consumption in  
379 the area. Nevertheless, the WWTP receives wastewater from nearby livestock husbandries,  
380 thus the veterinary-related load could be relevant and, currently, still unknown. In fact, in the  
381 early 1960s, SPY was the first macrolide intended for animal use (EMA, 2016). In EU, SPY  
382 use as growth promoter in feed was withdrawn in 1998 (Council Regulation (2821/98/EC),  
383 but it is still viable as therapeutic drug for cattle, poultry and pigs (Anadón et al., 2012).

384 Companies in EU are not required to provide background information about the amount of  
385 marketed veterinary drugs, thus the volume of used antibiotics is often very difficult to  
386 identify (EMA, 2016). Although data on antibiotics used on a species-by-species basis are  
387 rarely available, it is known that animal doses are significantly higher than humans (i.e. per  
388 unit of body weight) (EMA, 2016) explaining, at least in part, the amount of SPY detected in  
389 WWTP influent. The significant variation of antibiotics in influent during summer sampling  
390 could be due to many reasons, including antibiotics consumption pattern, seasonal and daily  
391 fluctuation of hydraulic loads.

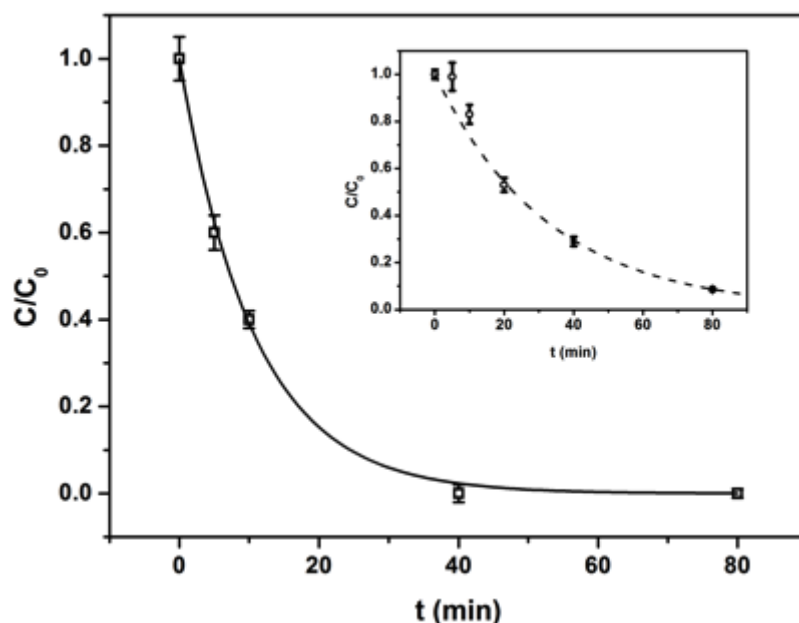
392 According to Table 1, SPY reduction rates ( $RR_W$ ) also varied seasonally from 9% in winter to  
393 >99.9% in summer. Zhou et al. (2013) reported that removal percentage for the macrolides in  
394 AS plants can vary from 8.79–89.4% which agrees well with our data. Any or very slight  
395 removal rates could be observed during winter season after both AS and at the final discharge.  
396 Accordingly, insufficient degradation of some macrolides, by AS processes was also reported  
397 by Birošová et al. (2016). In the summer period, SPY was completely removed already after  
398 the secondary treatment ( $RR_B$ ). In Beijing (China) WWTP, Li et al. (2013) stated that  
399 macrolides, including SPY, were persistent during conventional AS treatment (365 ng L<sup>-1</sup> in  
400 influents, 353 ng L<sup>-1</sup> in secondary effluents). Only after ultrafiltration coupled to ozonation,  
401 all target antibiotics were effectively reduced (from 85% up to >99.9%) decreasing their  
402 environmental risk.

403

### 404 **3.3 Photolysis and heterogeneous photocatalysis of SPY in real wastewater**

405 The photolysis of wastewater samples collected after the biological treatment during the  
406 summer period (SPY 5 µg/L) allowed to achieve >99.9% removal of SPY after 80 min  
407 (Figure 6). The degradation followed a PFO kinetic corresponding to a rate constant of  $0.094$   
408  $\pm 0.003$  min<sup>-1</sup> and a half-life ( $t_{1/2}$ ) of  $7.4 \pm 0.2$  min. Although the solar radiation is expected to  
409 be less efficient than UV one, these results could contribute to explain the high removal rate  
410 of SPY in WWTP during summer time.

411



412

413 **Figure 6** Photolysis of wastewater samples collected after the biological treatment during  
414 summer season (SPY 5 µg/L); (inlet) Photocatalysis with 0.1 g/L of TiO<sub>2</sub> of wastewater  
415 samples collected in winter season after biological treatment (SPY 30 µg/L); error bars  
416 represent standard error (n = 3).

417

418 When photocatalysis was carried out on the same wastewater samples with 0.1 g L<sup>-1</sup> of TiO<sub>2</sub>,  
419 a complete removal of SPY was attained only after 5 min. Thus, no kinetic study could be  
420 carried out. This result was attributed to the very low concentration of scavenger compounds  
421 in wastewater including organic substance (Table 1S), which made the hydroxyl radicals  
422 available for the oxidation of target pollutant. When photocatalysis was carried out in  
423 wastewater samples collected in winter season after the biological treatment (SPY 30 µg L<sup>-1</sup>),  
424 a reduction rate of 91% was achieved after 80 min of treatment (Figure 6 inlet).

425

### 426 3.2.4 Ecotoxicity

427 Results from quality assurance and quality control procedures were in line with the relative  
428 toxicity test protocols for both negative and positive controls. The effects of SPY to *V.*

429 *fischeri*, *R. subcapitata* and *D. magna* as EC5, EC20 and EC50 were reported in Table 3.  
430 Species presented a great range of sensitivities: *V. fischeri* < *D. magna* < *R. subcapitata*.  
431 Microalgae were the most sensitive biological model. SPY EC50 for *V. fischeri* was  
432 determined for the first time presenting no relevant effects, even though it has been already  
433 used for SPY contaminated wastewater sample assessment (Calza et al., 2010). SPY EC50 for  
434 *R. subcapitata* was like Halling-Sørensen (2000) (1.3-4.0 mg/L) and Minguez et al. (2016)  
435 (4.12-6.01 mg/L); SPY EC50 for *D. magna* was in accordance with Minguez et al. (2016) (>  
436 100 mg/L). Effective concentrations for all species were several times greater than the real  
437 detected SPY concentration in untreated wastewater (5-35  $\mu\text{g L}^{-1}$ , Table 1).  
438 The application of risk quotients considering the predicted environmental concentration  
439 (PEC) and predicted no effect concentration (PNEC) showed that SPY did not present any  
440 risk of direct toxicity, but the potentiality to induce antibiotic resistance cannot be considered  
441 in such traditional risk evaluation and are still under investigated.  
442 About SPY spiked samples, toxicity data were displayed considering single species effects in  
443 Figure 7; results were integrated according to Persoone et al. (2003) in Table 4. Outcomes  
444 from *V. fischeri* (15 min) (Figure 4 A) showed that toxicity was not significantly influenced ( $p$   
445 < 0.05) by the amount of  $\text{TiO}_2$  (0.1-4  $\text{g L}^{-1}$ ) used during the treatment process with an average  
446 residual toxicity of 7-18%.  
447 Data from *R. subcapitata* (15 min) (Figure 4 B) showed that toxicity was not significantly  
448 influenced ( $p$  < 0.05) by the amount of  $\text{TiO}_2$  (0.1-4  $\text{g L}^{-1}$ ) used during the process. Average  
449 residual toxicity was always > 40% and up to 52%; no EC50 values could be estimated.  
450 Daphnids evidenced a significant increasing toxicity trend in treated SPY solutions from 0.1  
451 to 4  $\text{g L}^{-1}$   $\text{TiO}_2$ , with an average residual effect always  $\geq$  13% (Figure 4 C).  
452 The toxicity of SPY spiked samples after treatment could be associated to SPY by-products  
453 that were not completely removed as previously described. Residual toxicity was not

454 satisfactorily reduced below 10% effect that is the commonly accepted “no effect” threshold  
455 in many toxicity tests considering negative controls (Lofrano et al., 2016b). Further  
456 optimization of the treatment process will be necessary to meet the goal of toxicity reduction  
457 up to < 10% effect.

458 About toxicity data ranking and integration (Persoone et al., 2003) (Table 4), effects were  
459 singly scored from *no acute hazard* (i.e. mainly due to *V. fischeri*), and *slight acute hazard*  
460 (i.e. mainly due to *D. magna*) to *acute hazard* (i.e. *R. subcapitata*). Integrated results  
461 supported the general issue related to the presence of residual slight acute hazard in treated  
462 samples without any distinction about the amount of TiO<sub>2</sub> used within the treatment process.

463 **Table 3** Toxicity effects of SPY on *V. fischeri* 15 min, *R. subcapitata* and *D. magna* 48 h as  
464 effective concentrations (EC) able to promote 5 (EC5), 20 (EC20) and 50% (EC50) effect.

	EC5	EC20	EC50
Species	mg L <sup>-1</sup>		
<i>V. fischeri</i> *	1348**	2944**	8263**
<i>R. subcapitata</i>	0.02 (0.09-0.03)	0.25 (0.16-0.36)	4.0 (3.2-5.0)
<i>D. magna</i> <sup>+</sup>	70 (37-99)	281 (257-304)	503 (478-530)

\*15 min; \*\* forecast values; <sup>+</sup>48 h

465

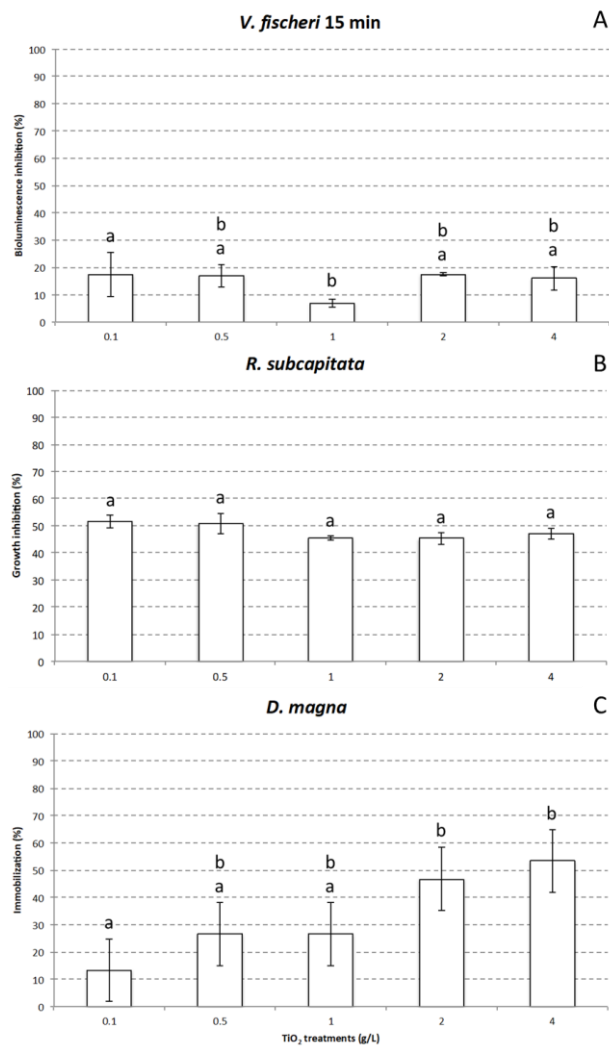
466

467

468

469

470



472

473 **Figure 7** Toxicity results of treated SPY solution (10 mg L<sup>-1</sup>) after 0.1, 0.5, 1, 2 and 4 g L<sup>-1</sup> of  
 474 TiO<sub>2</sub> including *V. fischeri* bioluminescence inhibition after 15 min (A) contact time, *R.*  
 475 *subcapitata* growth inhibition (B), and *D. magna* mortality after 48 h (C) contact time; data  
 476 with different letters (a–b) are significantly different (Tukey's, p < 0.05); error bars represent  
 477 standard error (n = 3).

	nTiO <sub>2</sub> (mg/L)											
	0.1		0.5		1		2		4			
Very high acute hazard												
High acute hazard												
Acute hazard		2		2							2	
Slight acute hazard				1		1	1		1	1		1
No acute hazard	0		0	0		0			0			0

Final class weight score	1	1	1	1	1


  
 V. fischeri 15 min  
 R. subcapitata  
 D. magna 48 h

478

479

480 **Table 4** Integrated assessment of toxicity data from treated (0.1, 0.5, 1, 2 and 4 mg L<sup>-1</sup> of  
 481 TiO<sub>2</sub>) SPY solutions including *V. fischeri* 15 min, *R. subcapitata* and *D. magna* 48 h  
 482 according to Persoone et al. (2003) toxicity class weight score for the classification of natural  
 483 waters.

484

485

486 **4. Conclusions**

- 487 • The antibiotic concentration in municipal wastewater can significantly vary on a  
488 seasonal basis and between different WWTPs; therefore, a preliminary monitoring is  
489 necessary for a proper management strategy on a case-by-case basis;
- 490 • The photocatalytic process showed to be very efficient in SPY removal (> 90%) also  
491 at relatively high concentrations as those detected in the monitored WWTP compared  
492 to conventional AS treatments;
- 493 • The optimal range of TiO<sub>2</sub> concentration must be determined time-by-time to avoid  
494 the use of an excess of the reactive agent ensuring that the absorption of radiation  
495 photons is maximized for an efficient degradation;
- 496 • Acute effects were still present in treated effluents up to more than 50%. Further  
497 optimization of the process is necessary to meet the goal of reducing toxicity < 10%  
498 threshold effect.

499

500

501

502 **References**

503 Al-Rifai, J. H., Khabbaz, H., Schäfer, A. I., 2011. Removal of pharmaceuticals and endocrine  
504 disrupting compounds in a water recycling process using reverse osmosis systems. *Separation  
505 and Purification Technology*, 77(1), 60-67.

506

507 Anadón, A., Martínez-Larrañaga, M. R., Castellano, V., 2012. Regulatory aspects for the  
508 drugs and chemicals used in food-producing animals in the European Union. *Veterinary  
509 Toxicology: Basic and Clinical Principles*, 135.

510

511 APHA, 2012. American Public Health Association, American Water Works Association,  
512 Water Environment Federation, Standard Methods, 2012. E.W. Rice, R.B. Baird, A.D. Eaton,  
513 L.S. Clesceri, editors.

514

515 Batt, A. L., Kim, S., Aga, D. S., 2007. Comparison of the occurrence of antibiotics in four  
516 full-scale wastewater treatment plants with varying designs and operations. *Chemosphere*,  
517 68(3), 428-435.

518

519 Benotti, M. J., Trenholm, R. A., Vanderford, B. J., Holady, J. C., Stanford, B. D., Snyder, S.  
520 A. (2008). Pharmaceuticals and endocrine disrupting compounds in US drinking water.  
521 *Environmental science & technology*, 43(3), 597-603.

522

523 Birošová, L., Mackuľak, T., Bodík, I., Ryba, J., Škubák, J., Grabic, R., 2014. Pilot study of  
524 seasonal occurrence and distribution of antibiotics and drug resistant bacteria in wastewater  
525 treatment plants in Slovakia. *Science of The Total Environment*, 490, 440-444.

526

527 Chekir, N., Laoufi, N. A., Bentahar, F., 2014. Spiramycin photocatalysis under artificial UV  
528 radiation and natural sunlight. *Desalination and Water Treatment*, 52(34-36), 6832-6839.  
529

530 Calza P., Marchisio S., Medana C., Baiocchi C., 2010. Fate of antibacterial spiramycin in  
531 river waters. *Anal Bioanal Chem* 396:1539–1550.  
532

533 Carotenuto M., Lofrano G., Siciliano A., Aliberti F., Guida M., 2014. TiO<sub>2</sub> photocatalytic  
534 degradation of caffeine and ecotoxicological assessment of oxidation by-products. *Global*  
535 *Nest Journal* 16 (3), 265-275  
536

537 De Luca A., Falcao Dantas R., Simoes A.S. M., Salata Toscano I. A., Lofrano G., Cruz A.,  
538 Esplugas S., 2013. Atrazine removal in municipal secondary effluents by Fenton and photo-  
539 Fenton treatments. *Chemical Engineering & Technology* 36: 1-9.  
540

541 ECDC, 2014. Antimicrobial resistance surveillance in Europe. Annual report of the European  
542 Antimicrobial Resistance Surveillance Network (EARS-Net)  
543

544 EMA, 2016. Sales of veterinary antimicrobial agents in 26 EU/EEA countries in 2013  
545

546 Ferro, G., Fiorentino, A., Alferez, M. C., Polo-López, M. I., Rizzo, L., Fernández-Ibáñez, P.,  
547 2015. Urban wastewater disinfection for agricultural reuse: effect of solar driven AOPs in the  
548 inactivation of a multidrug resistant *E. coli* strain. *Applied Catalysis B: Environmental*, 178,  
549 65-73.  
550

551 Gracia-Lor, E., Sancho, J. V., Serrano, R., Hernández, F., 2012. Occurrence and removal of  
552 pharmaceuticals in wastewater treatment plants at the Spanish Mediterranean area of  
553 Valencia. *Chemosphere*, 87(5), 453-462.

554

555 Halling-Sørensen B., Algal toxicity of antibacterial agents used in intensive farming, In  
556 *Chemosphere*, 40(7), 731-739.

557

558 Hatchard, C. G., Parker, C. A., 1956. A new sensitive chemical actinometer. II. Potassium  
559 ferrioxalate as a standard chemical actinometer. In *Proceedings of the Royal Society of*  
560 *London A: Mathematical, Physical and Engineering Sciences* (Vol. 235, No. 1203, pp. 518-  
561 536). The Royal Society.

562

563 Kim, S., Aga, D.S., 2007. Potential ecological and human health impacts of antibiotics and  
564 antibiotic-resistant bacteria from wastewater treatment plants. *J. Toxicol. Environ. Health B*  
565 10, 559–573.

566

567 ISO (International Organisation for Standardisation, Geneva, Switzerland), 2007. *Water*  
568 *Quality – Determination of the Inhibitory Effect of Water Samples on the Light Emission of*  
569 *Vibrio fischeri* (Luminescent bacteria test) – Part 3:Method Using Freeze-Dried Bacteria.

570

571 ISO, 2012. *Water Quality – Freshwater Algal Growth Inhibition Test with Unicellular Green*  
572 *Algae*. 8692. ISO, Geneva 2012.

573

574 ISO, 2013. *Water Quality: Determination of the Inhibition of the Mobility of Daphnia magna*  
575 *Straus* (Cladocera, Crustacea) – Acute Toxicity Test.

576

577 Jelić, A., Petrović, M., Barceló, D., 2009. Multi-residue method for trace level determination  
578 of pharmaceuticals in solid samples using pressurized liquid extraction followed by liquid  
579 chromatography/quadrupole-linear ion trap mass spectrometry. *Talanta*, 80(1), 363-371.

580

581 Li, B., Zhang, T., 2011. Mass flows and removal of antibiotics in two municipal wastewater  
582 treatment plants. *Chemosphere*, 83(9), 1284-1289.

583

584 Li, W., Shi, Y., Gao, L., Liu, J., Cai, Y., 2013. Occurrence, distribution and potential affecting  
585 factors of antibiotics in sewage sludge of wastewater treatment plants in China. *Science of the*  
586 *total environment*, 445, 306-313.

587

588 Libralato G., Volpi Ghirardini A., Avezzù F., 2010. How toxic is toxic? A proposal for  
589 wastewater toxicity hazard assessment. *Ecotoxicology and Environmental Safety* 73, 1602-  
590 1611. doi: 10.1016/j.ecoenv.2010.03.007

591

592 Libralato G., Avezzù F., Volpi Ghirardini A., 2011. Lignin and tannin toxicity to  
593 *Phaeodactylum tricornutum* (Bohlin). *Journal of Hazardous Materials* 194, 435–439.

594

595 Lofrano G., Libralato G., Carotenuto M., Guida M., Inglese M., Siciliano A., Meriç S., 2016a.  
596 Emerging Concern from Short-Term Leaching: A Preliminary Ecotoxicological Survey.  
597 *Bulletin of Environmental Contamination and Toxicology* 97, 646-652

598

599 Lofrano G., Libralato G., Adinolfi R., Siciliano A., Iannece P., Guida M., Giugni M., Volpi  
600 Ghirardini A., Carotenuto M., 2016b. Photocatalytic degradation of the antibiotic

601 chloramphenicol and its by-products toxicity effects. *Ecotoxicology and Environmental*  
602 *Safety* 123, 65-71.

603

604 Lofrano G., Pedrazzani R. Libralato G., Carotenuto M., 2017. Advanced oxidation processes  
605 for antibiotic removal: a review. *Current Organic Chemistry*, in press

606

607 Malato, S., Blanco, J., Vidal, A., Richter, C. (2002). Photocatalysis with solar energy at a  
608 pilot-plant scale: an overview. *Applied Catalysis B: Environmental*, 37(1), 1-15.

609

610 Maselli, V., Siciliano, A., Giorgio, A., Falanga, A., Galdiero, S., Guida, M., Fulgione, D.,  
611 Galdiero, E., 2017. Multigenerational effects and DNA alterations of QDs-Indolicidin on  
612 *Daphnia magna*. *Environmental Pollution*, 224, 597-605.

613

614 McArdell, C. S., Molnar, E., Suter, M. J. F., Giger, W. (2003). Occurrence and fate of  
615 macrolide antibiotics in wastewater treatment plants and in the Glatt Valley Watershed,  
616 Switzerland. *Environmental Science & Technology*, 37(24), 5479-5486.

617

618 Michael I., Rizzo L., McArdell C.S., Manaia C.M., Merlin C., Schwartz T., Dagot C., Fatta-  
619 Kassinos D., 2013. Urban wastewater treatment plants as hotspots for the release of  
620 antibiotics in the environment: a review. *Water Research*, 47:957–95.

621

622 Minetto D., Volpi Ghirardini A., Libralato G., 2016. Saltwater ecotoxicology of Ag, Au,  
623 CuO, TiO<sub>2</sub>, ZnO and C<sub>60</sub> engineered nanoparticles: an overview. *Environment International*  
624 92-93, 189-201.

625

- 626 Minguez, L., Pedelucq, J., Farcy, E., Ballandonne, C., Budzinski, H., Halm-Lemeille, M. P.,  
627 2016. Toxicities of 48 pharmaceuticals and their freshwater and marine environmental  
628 assessment in northwestern France. *Environmental Science and Pollution Research*, 23(6),  
629 4992-5001.
- 630
- 631 Persoone, G., Marsalek, B., Blinova, I., Törökne, A., Zarina, D., Manusadzianas, L., Nalecz-  
632 Jawecki G., Tofan L., Stepanova N., Tothova L., Kolar, B. (2003). A practical and  
633 user-friendly toxicity classification system with microbiotests for natural waters and  
634 wastewaters. *Environmental Toxicology*, 18(6), 395-402.
- 635
- 636 Pomati, F., Castiglioni, S., Zuccato, E., Fanelli, R., Vigetti, D., Rossetti, C., Calamari, D.,  
637 2006. Effects of a complex mixture of therapeutic drugs at environmental levels on human  
638 embryonic cells. *Environ. Sci. Technol.* 40, 2442–2447.
- 639
- 640 Pomati, F., Cotsapas, C.J., Castiglioni, S., Zuccato, E., Calamari, D., 2007. Gene expression  
641 profiles in zebrafish (*Danio rerio*) liver cells exposed to a mixture of pharmaceuticals at  
642 environmentally relevant concentrations. *Chemosphere* 70, 65-73.
- 643
- 644 Rasheed, T., Bilal M., Iqbal, H. M. N., Hu, H., Zhang, X., 2017a. Reaction Mechanism and  
645 Degradation Pathway of Rhodamine 6G by Photocatalytic Treatment. *Water, Air, & Soil*  
646 *Pollution*, 228(8), 291
- 647
- 648 Rasheed, T., Bilal M., Iqbal, H. M. N., Hu, H., Zhang, X., Zhou Y., 2017b. TiO<sub>2</sub>/UV-assisted  
649 Rhodamine B degradation: putative pathway and identification of intermediates by  
650 UPLC/MS. *Environmental Technology*, 31, 1-11.

651

652 Sarmah, A. K., Meyer, M. T., & Boxall, A. B., 2006. A global perspective on the use, sales,  
653 exposure pathways, occurrence, fate and effects of veterinary antibiotics (VAs) in the  
654 environment. *Chemosphere*, 65(5), 725-759.

655

656 Vaiano V., Sacco O., Sannino D., Ciambelli P., Nanostructured N-doped TiO<sub>2</sub> coated on glass  
657 spheres for the photocatalytic removal of organic dyes under UV or visible light irradiation,  
658 2015. *Applied Catalysis B: Environmental*, 170-171, 153-161.

659

660 Van Boeckel, T.P., Brower, C., Gilbert, M., Grenfell, B.T., Levin, S.A., Robinson, T.P.,  
661 Laxminarayan, R., 2015. Global trends in antimicrobial use in food animals. *Proc. Natl. Acad.*  
662 *Sci. U. S. A.* 112 (18), 5649-5654.

663

664 Zhou L-J, Ying GG, Liu S, Zhao JL, Zang B, Chen ZF, Lai H.J., 2013. Occurrence and fate of  
665 eleven classes of antibiotics in two typical wastewater treatment plants in South China.  
666 *Science of the Total Environment*, 452-453, 365-376.

667

668 Zuccato, E., Castiglioni, S., Fanelli, R., 2005. Identification of the pharmaceuticals for human  
669 use contaminating the Italian aquatic environment. *Journal of Hazardous Materials*, 122(3),  
670 205-209.

671

672 Zuccato, E., Castiglioni, S., Bagnati, R., Melis, M., Fanelli, R., 2010. Source, occurrence and  
673 fate of antibiotics in the Italian aquatic environment. *Journal of Hazardous Materials*, 179(1),  
674 1042-1048.

675

676 Wilson, B.A., Smith, V.H., Denoyelles, F., Larive, C.K., 2003. Effects of three  
677 pharmaceutical and personal care products on natural freshwater algal assemblages.  
678 *Environmental Science & Technology*, 37, 1713–1719.

679

680 Wang, M., Tang, J.C., 2010. Research of antibiotics pollution in soil environments and its  
681 ecological toxicity. *Journal of Agro-Environment Science*, 29, 261-266.

682

683 Watkinson, A. J., Murby, E. J., Costanzo, S. D., 2007. Removal of antibiotics in conventional  
684 and advanced wastewater treatment: implications for environmental discharge and wastewater  
685 recycling. *Water Research*, 41(18), 4164-4176.

686

687 Watch List (2015). Decision, E. U. 495/2015, Commission Implementing Decision (EU)  
688 2015/495 of 20 March 2015 establishing a watch list of substances for Union-wide  
689 monitoring in the field of water policy pursuant to Directive 2008/105/EC of the European  
690 Parliament and of the Council. *Off. J. Eur. Union L*, 78, 40-42.

691

692

693 **Captions figures**

694

695 **Figure 1** HPLC chromatogram of SPY - inlet: UV spectra of SPY.

696

697 **Figure 2** Photocatalytic kinetic curves of SPY (10 and 70 mg L<sup>-1</sup>) after 5, 20, 40, 80 min at  
698 0.1 g L<sup>-1</sup> of TiO<sub>2</sub> at pH 5.5; error bars represent standard error (n = 3).

699

700 **Figure 3** Photocatalytic kinetic curves of SPY (10 mg L<sup>-1</sup>) after 5, 10, 20, 40, 80 min at 0.1,  
701 0.5, 1.0, 2.0, 4.0 g L<sup>-1</sup> of TiO<sub>2</sub> at pH 5.5; error bars represent standard error (n = 3).

702

703 **Figure 4** ESI-MS spectra in positive ion mode on untreated SPY (70 mgL<sup>-1</sup>) (a), SPY  
704 photocatalysis (70 mgL<sup>-1</sup>) at 0.1 gL<sup>-1</sup> of TiO<sub>2</sub> after 10 min (b), 20 min (c) and 80 min (d);  
705 \*SPY and \*\* [SPY + CH<sub>3</sub>COOH] formed during the injection phase in ESI-MS.

706

707 **Figure 5** Molecules associated to the peaks identified in Figure 4.

708

709 **Figure 6** Photolysis of wastewater samples collected after the biological treatment during  
710 summer season (SPY 5 µg/L); inlet Photocatalysis with 0.1 g/L of TiO<sub>2</sub> of wastewater  
711 samples collected in winter season after biological treatment (SPY 30 µg/L); error bars  
712 represent standard error (n = 3).

713

714 **Figure 7** Toxicity results of treated SPY solution (10 mg L<sup>-1</sup>) after 0.1, 0.5, 1, 2 and 4 g L<sup>-1</sup> of  
715 TiO<sub>2</sub> including *V. fischeri* bioluminescence inhibition after 15 min (A) contact time, *R.*  
716 *subcapitata* growth inhibition (B), and *D. magna* mortality after 48 h (C) contact time; data  
717 with different letters (a–b) are significantly different (Tukey's, p < 0.05).

718 **Captions of tables**

719

720 **Table 1** Occurrence of SPY in WWTP (Campania, Italy) before (influent), after activated  
721 sludge (AS) biological treatment and at the final discharge point (effluent); SPY reduction  
722 rates (%) were reported within the same season ( $RR_W$  = Reduction Rate influent-effluent) and  
723 between winter- and summertime ( $RR_B$ ).

724

725 **Table 2** Half-life ( $t_{1/2}$ ) of SPY ( $10 \text{ mg L}^{-1}$ ) and the pseudo first order constant ( $k$ ).

726

727 **Table 3** Toxicity effects of SPY on *V. fischeri* 15 min, *R. subcapitata* and *D. magna* 48 h as  
728 effective concentrations (EC) able to promote 5 (EC5), 20 (EC20) and 50% (EC50) effect.

729

730 **Table 4** Integrated assessment of toxicity data from treated ( $0.1, 0.5, 1, 2$  and  $4 \text{ min g L}^{-1}$  of  
731  $\text{TiO}_2$ ) SPY solutions including *V. fischeri* 15 min, *R. subcapitata* and *D. magna* 48 h  
732 according to Persoone et al. (2003) toxicity class weight score for the classification of natural  
733 waters.

734

735

736

**Supplementary material for on-line publication only**

**[Click here to download Supplementary material for on-line publication only: Table 1S.docx](#)**

<https://doi.org/10.1016/j.scitotenv.2017.12.145>